

Andrew Niehaus

GEOG 322

Professor Karen Frey

16 December 2023

Explorating Statistical Methods in Melt Season Detection with Radar Data

Abstract

Glacial melt is a key indicator of climatological patterns with important implications of increased melt such as changes to local ecosystems, changes to local climate regulation, and contribution to sea level rise. Rising temperatures produce longer and more intense melt seasons in glaciated areas, strengthening effects of the described consequences. Scatterometer data collected in the microwave band serves as a useful method in studying glacial melt due to its temporal resolution and sensitivity to standing water on ice and snow, allowing detection of surface melt on glaciers.

Literature such as Trusel 2012, Wang 2008, and Panday 2011 serve as examples of this methodology on the Arctic, the Antarctic, and the Himalayan Mountain Region. These studies estimate melt season length using a combination of scatterometer data as well as in situ meteorological station temperature data, which helps inform backscatter thresholds used to detect melt seasons. Such methodology restricts potential study sites to areas closely surrounding such meteorological stations. In the interest of developing a methodology that is suitable for a greater spatial range of sites, this study develops a process to characterize inter-annual and seasonal melt season patterns in glaciated areas in the absence of in situ meteorological station data.

This is done with three time series of 2007-2022 ASCAT scatterometer data at a bi-daily observational frequency. Yearly melt seasons are measured for each site and are studied in their timing, duration, variance, magnitude, and interannual patterns. This study explores the use of statistical measurements and metrics in melt season characterization in ways that have been rarely observed in existing literature and deepens the potential for characterization and comparison of glacial melt season patterns. With the utility of this study, climatological relationships with glaciers in the Arctic, Antarctic, and Himalayan Mountain Region as well as smaller glacier systems can be better understood and subsequently incorporated into studies and climate models.

Introduction

Glacial melt is a central consequence of rising temperatures from climate change. Understanding melt season patterns in glaciated regions has multiple relevant applications including as an indicator of larger climatological trends, as a driver of local water supply dynamics, and as a central force in local ecology. As climate monitoring becomes increasingly relevant to our understanding of climate change, glacial melt season detection serves as a key method to understand seasonal and inter-annual trends. Literature such as Trusel (2012), Alley et. al (2018), Rawlins et. al (2005), Arndt et. al (1994), and Panday et. al, (2011) provides great examples of such research on a range of applications.

Scatterometer data analysis is one of the most widely used methods in melt season detection. This is done in microwave frequencies, which are particularly sensitive to frozen vs. partially melted surfaces. Studies such as INSERT serve as precedent in this analysis, primarily covering the Arctic and Antarctic in their study areas. Methodology for melt season detection

with scatterometer data is explained accessibly in (Trusel et. al (2012) and Panday et. al (2011). The process hinges on the creation of a melt season threshold for backscatter values- such that backscatter values below the threshold qualify as melt days. This threshold must be created individually to each site to isolate melt as patterns relative to yearly local backscatter, rather than using universal backscatter values to define melt. This threshold is commonly calculated through the subtraction of a user-defined constant from a mean winter backscatter for that year. The threshold constant is defined through an inspection of backscatter patterns along with local temperature data to the study area, acquired from meteorological stations in projects such as the NOAA's Global Summary of Day (GSOD) or the NCAR's Coordinated Enhanced Observing Period (CEOP).

This traditional methodology of melt season detection allows for high quality analysis of study areas it is used on, but limits the range of potential study areas to the local space around high temporal resolution meteorological stations with up to date data availability. This study aims to experiment in the process of melt season detection with scatterometer data with a lack of in situ meteorological station temperature data. This difference in methodology decreases the precision in melt season detection, but increases the geographic range melt season detection can be run on.

Methods

Study Site

Three sites were chosen for the study spanning the Eastern Himalayan region; in Nepal, Bhutan, and China. The sites (shown in figures 1-3) cover high elevation glaciers dominated by snow cover. Each site was created as a 8.9 km by 8.9 km square, based on the 4.45 km by 4.45

km pixel size of the acquired ASCAT data. Scatterometer data was extracted from the NASA Scatterometer Climate Record Pathfinder (SCP) project at a bi-daily frequency for the 2007-2022 time series. Mean backscatter values were extracted for each study site using the Earth Trend Modeler in Terrset.

Scatterometer data download and extraction

With extraction complete, the time series of backscatter values was moved into Microsoft Excel for statistical analysis. Yearly summary statistics were first calculated such as mean, standard deviation, maximum three day average, and minimum three day average. Maximum and minimum three day averages were used to estimate the range and intensity of backscatter patterns in a more standardized context than single day values given the potential for mechanical error or inaccuracy.

Threshold Constant Setting

Antarctic surface melting dynamics: Enhanced perspectives from radar scatterometer data by Trusel, et. al (2012) was used a central precedent for the methodology in this study. Trusel's work establishes a thresholding technique in detecting melt seasons that relies on in situ meteorological station temperature data to calibrate a threshold formula which is unique to the data patterns of the study site in the year in question. High temporal resolution temperature data is used to establish the point of melt season onset in backscatter by lining up with temperature increases above 0 degrees Celsius. As discussed, this study did not use in situ meteorological station but rather used a visual inspection of backscatter plots in relation to threshold constants shown in Figures 10-12 to best isolate melt signal.

Threshold constants were first explored as shown in figures (10-12). Melt season lengths across threshold constants from 0.25 to 2.5 decibels on 0.25 decibel thresholds displayed behavior approximately linear and did not have any noticeable changes in their large trends at specific threshold constants.

The lack of noticeable departures from general trends in the detected melt season length across threshold constant forced the decision of constant to rely heavily on visual examination. This decision was made with a goal of capturing melt signals without noise at the start and end of the season- coming in the form of values oscillating above and below the threshold. Threshold constants for Sagarmatha, Nyingchi, and Lunana were set at 1, 1.25, and 1.5 respectively.

In addition to a visual inspection, these threshold constants were informed by a study of backscatter variability over the 16 year series. Lunana had the greatest deviation of the three sites, Sagarmatha had the least, and Nyingchi was in the middle. Melt season threshold constants reflect this- with the intention to have threshold constants reflect the respective sites in relation to each other.

Melt Season Detection

Once threshold constants were set, melt season start and end dates were set through a similar process. The study was designed for the subject of melt season patterns observed in backscatter, thus melt seasons were recorded to favor quality of signal over capturing all possible melt. Melt seasons were then analyzed for patterns in onset date, freeze-up date, and length. Melt onset and freeze-up dates were used to divide each year into three seasons: pre-melt, melt, and post-melt. These sub seasons were separated for further analysis.

Melt Season Backscatter Variance and Days of Large Change

In addition to the timing and length of respective seasons, it is relevant to consider the magnitude of behaviors across years and across sites. This was done by recording the range of backscatter within melt seasons as well as counts of *large change days*. These are defined as observations whose backscatter differs by more than 0.5, 0.425, and 0.35 decibels from the previous observation for Lunana, Nyingchi, and Sagarmatha respectively. This pattern was established to mimic the pattern of threshold constants stemming from the variance of each site.

Results

Summary Statistics

Lunana and Nyingchi sites show similar high level patterns of variance while Sagarmatha shows noticeably lower backscatter values with less variation. As seen in histograms, Lunana has unimodal backscatter value distribution with its peak at low backscatter values, while Nyingchi and Sagarmatha have bimodal distributions with peaks at both low and high backscatter values. Lunana and Sagarmatha are skewed towards lower backscatter values while Nyingchi is skewed towards higher backscatter values. Mean three day maximum backscatter values show greater variance than mean three day minimum backscatter values in all three sites.

Melt Season Timing and Duration

Melt season length across threshold constants shows some outlier years within sites (Nyingchi 2007, Lunana 2015, and to a lesser degree Sagarmatha 2009), but does not show any critical threshold constant values to create a natural breaking point in measurements. Detected melt days display approximately linear relationships with threshold constant values in each site.

Threshold constants of 1, 1.25, and 1.5 were set for Sagarmatha, Nyingchi, and Lunana respectively based on patterns of variance between the three sites as well as visual inspections.

Subsequent melt season duration calculations validate the observed differences between backscatter value patterns in Lunana, Nyingchi, and Sagarmatha; Nyingchi has noticeably longer melt seasons than the other two study sites. All three sites follow a predominantly oscillatory pattern, with Nyingchi and Sagarmatha trending towards slightly longer melt seasons. Figure 6 display the raw backscatter values for each melt season. These charts reveal a notable pattern in the Nyingchi melt seasons as their backscatter values increase at comparable times of the year to the other two sites, but then decrease in the middle of the apparent melt season, before increasing again and subsequently following typical freeze-up patterns. These charts also visualize the previously mentioned outlier melt seasons- Nyingchi 2007, Lunana 2015, and Sagarmatha 2009. Interestingly, these outlier seasons tend to depart from site trends in the direction of lower backscatter values, rather than higher backscatter values- suggesting colder seasons and less melt.

An inspection of a visualization of melt onset and freeze-up dates again separates Nyingchi with different tendencies than Lunana and Sagarmatha. Nyingchi shows greater variance in its freeze-up dates than its melt onset dates, while Lunana and Sagarmatha show greater variance in their melt onset dates than their freeze-up dates. Additionally, Lunana and Sagarmatha show nearly identical mean freeze-up dates- however Sagarmatha has a mean melt onset date 11 days earlier than Lunana. Pre/post backscatter peak melt length charts display some notable differences in behavior between sites. Nyingchi shows the greatest variance in pre/post backscatter peak melt length with percentages ranging from 20 to 80 on either side- 20% of the melt season occurring before the peak 3 day average or 80% of the melt season occurring before

the peak 3 day average. Lunana shows more variance than Sagarmatha, but tends towards lower pre peak percentages; thus more of the melt season occurring after the peak backscatter.

Melt Season Intensity

Melt Season variance was calculated as the range for backscatter values in the melt season yearly by site. The visualization of this data in Figure 31 shows Lunana and Nyingchi having similar melt season backscatter variance, while Sagarmatha has a notably lower yearly variance. The three sites do not show any notable inter-annual trends. Large change days were defined as days greater or less than the previous days backscatter by 0.5, 0.425, and 0.35 decibels for Lunana, Nyingchi, and Sagarmatha respectively, which was calculated to match the pattern of threshold constants for each site following the different degrees of variance.

Discussion

Interannual and cross-site trends of summary statistics

The three study sites display notably different patterns in their summary statistics as well as more detailed analysis techniques. Figure 6 illustrates similar patterns of backscatter range and deviation patterns in Lunana and Sagarmatha, but contrary patterns to these two sites in Nyingchi. A possible contributing factor to this is Nyingchi's elevation, which is lower than that of Lunana and Sagarmatha (Figure 4). Nyingchi and Lunana display similar patterns to each other in magnitude of deviation while Sagarmatha's magnitude of deviation is notably lower. Backscatter value distributions for each site (Figures BLANK through BLANK) reveal a new pattern of bimodality in Nyingchi and Sagarmatha and unimodality in Lunana. This brings into

question the nature of pure melt signal backscatter values and what separates the Lunana site from Nyingchi and Sagarmatha.

It is also noticeable from the 16 year backscatter plots (Figure 6) that Nyingchi and Lunana have similar maximum backscatter values (Lunana's are lower by about 1 decibel) but Lunana's minimum backscatter values are further from Nyingchi's minimums than the difference in maximums. While not describing much yet about specific melt season behaviors, these summary statistics begin to paint the picture of each of these sites having unique backscatter patterns.

Thresholding and melt season lengths

The threshold constant testing and subsequent decision were the weakest aspect of this methodology and the experience the most notable effect from the lack of in situ meteorological station data. As shown in Figures 10-12, there is no natural forming threshold which changes the melt signal- increasing the threshold constant decreases the detected melt season on a generally linear pattern for each site. The logic for each site's threshold constant was thus based on the variance each site displayed - where sites with more variance should theoretically necessitate larger threshold constants to isolate the melt signal. Additionally, the method of assigning a melt onset and freeze up date to each was not a precise process- it was performed qualitatively with the intent being to find the date where the backscatter crossed the threshold without going back above/below it for the rest of the year. This could be addressed through a bit of programming in the melt season detection process, which was out of the scope for this study.

The detected melt season lengths do not show any inter-annual trends and generally oscillate within a 30 day range for the 16 year time series. This pattern is broken a few times by

outlier years, most predominantly Nyingchi 2007 which has a melt season half the length of detected seasons through the rest of the series. 2007 has shorter melt seasons for the other sites as well, but not nearly to the degree Nyingchi experiences. This suggests a local climatological dynamic that year which could be explored in future studies.

Melt season timing analysis

Figures 18-20 visualize the start and end of melt seasons for each site and Figure 21 shows some summary statistics of onset and freeze-up dates. This again demonstrates the longer melt seasons and greater deviation of Nyingchi as well as the similarity between Lunana and Sagarmatha. The pattern of earlier melt onset dates in Sagarmatha but similar freeze-up dates are interesting and provide another opportunity for further analysis to investigate what climatological factors or local characteristics might drive this dynamic. Pre/post backscatter peak melt season ratios provide a unique perspective to melt season behavior in the three sites, normalizing the length of melt season before the maximum three day average backscatter and after to the individual length of melt season in a given year, giving context to the timing of peak melt within melt seasons. All three sites show an overall pattern of shorter pre peak melt seasons than post peak melt seasons, but show different levels of variance within this pattern. Nyingchi has notably large pre peak melt seasons in 2007, 2008, 2010, 2016, 2018, and 2020. Sagarmatha shows the most consistent signal of pre/post peak melt season ratio, with only two years surpassing 50% pre peak melt season length. These observed trends suggest a quicker transition from the beginning of melt season to peak melt than from peak melt to freeze-up. This can also be observed in the raw backscatter data which show a lower slope in the progression towards freeze-up than following melt onset. Timing of peak melt can have key impacts on the region

surrounding a glaciated area, and the implications of changes of this dynamic are a key topic to be studied further.

Melt season intensity analysis

Melt season intensity was visualized primarily through melt season backscatter range charts (Figure 31). This shows notably similar trends to melt season lengths in Figure 14, suggesting longer melt seasons correlate with greater peak intensity. In contrast to the visualization of melt season length, however, peak intensity shows Lunana and Nyingchi having similar magnitudes with Sagarmatha being much lower. This depicts Lunana in an interesting context in which it has shorter melt seasons than Nyingchi, but similar peak intensities.

Limitations

This study had a few limitations, which were considered as part of the value of this research: to explore what could be found from analysis of melt season dynamics in the context of the given constraints on the project. In situ meteorological station data is preferable in the detection of glacial melt seasons to create an understanding of ground truth climate conditions to calibrate melt threshold calculations with. As shown in this study, glaciated areas can have many different differences in seasonal backscatter patterns, and ground truth data assists in teasing many dynamics apart to isolate real melt.

Future Direction

There are two primary paths of future direction for this topic. The first is pursuing methods to explore the relationship between melt season patterns and other local climatological

dynamics such as river flow volume, vegetation presence and intensity, or weather patterns such as monsoon seasons and their corresponding intensity. This could explore both causes and effects of melt season patterns by overlaying climatological data series on melt season lengths or other metrics shown in this study, or zoom in to outlier years or events and consider such parameters in the context of departures from larger melt season patterns.

Another path to future analysis which could be taken is to explore melt season characterization metrics and analysis further, through correlation analysis, change point detection, harmonic regression, or integration of backscatter values, among many other possible methods. Correlation analysis can identify relationships within the metrics used in this study and further inform an understanding of melt season patterns. Change point detection could expand the understanding of seasonal backscatter patterns as they relate to melt- illuminating local trends and events that may not otherwise be detectable. Harmonic regression can better model and visualize melt season backscatter behavior and identify departures from such behavior. Finally, the integration of melt season backscatter values more precisely and accurately quantifies melt season intensity than the methods used in this study. Intensity of melt is equally as relevant to the implications of glacial melt patterns as the season length and a quantification of intensity would provide notable insights into melt season characteristics and behaviors.

Finally, a key future direction with this research is to apply it to more glaciated areas. The metrics calculated and shown in this study have the potential to provide incredible insight to interannual and seasonal trends in glacial melt seasons. Existing literature does not provide a large selection of research showing similar quantifications of melt season dynamics. As behaviors of these metrics become more established over larger spatial and temporal ranges,

subsequent studies will be able to better characterize melt season dynamics of individual study sites.

Conclusion

This study explored methods of glacial melt season characterization with scatterometer time series data in the absence of in situ meteorological station data for three 8.9 km by 8.9 km squares in the Himalayan Mountain Region from 2007-2022. The three sites showed differences and similarities with one another in different metrics and visualizations, suggesting deeper patterns of backscatter behavior in relation to melt and climate which are not fully understood yet. The methods shown and discussed in this study provide an opportunity for more research of inter-annual and seasonal glacial melt season backscatter characteristics to better understand drivers of the metrics explored here. This research aims to expand the role of statistical methods used in glacial melt season detection and subsequently expand the applicability of such analysis into larger scope research such as climate modeling or hydrologic dynamic analysis.

References

- Alley, K. E., Scambos, T. A., Miller, J. Z., Long, D. G., & MacFerrin, M. (2018). Quantifying vulnerability of Antarctic ice shelves to hydrofracture using microwave scattering properties. *Remote Sensing of Environment*, 210, 297–306. <https://doi.org/10.1016/j.rse.2018.03.025>
- Arndt, S., & Haas, C. (2019). Spatiotemporal variability and decadal trends of snowmelt processes on Antarctic sea ice observed by satellite scatterometers. *The Cryosphere*, 13(7), 1943–1958. <https://doi.org/10.5194/tc-13-1943-2019>
- De Freitas, M. W. D., Mendes Júnior, C. W., Arigony-Neto, J., Costi, J., & Simões, J. C. (2018). A multiscale subpixel mixture analysis applied for melt detection using passive microwave and radar scatterometer image time series of the Antarctic Peninsula (1999–2009). *Annals of Glaciology*, 59(76pt1), 16–28. <https://doi.org/10.1017/aog.2017.44>
- Howell, S. E. L., Small, D., Rohner, C., Mahmud, M. S., Yackel, J. J., & Brady, M. (2019). Estimating melt onset over Arctic sea ice from time series multi-sensor Sentinel-1 and RADARSAT-2 backscatter. *Remote Sensing of Environment*, 229, 48–59. <https://doi.org/10.1016/j.rse.2019.04.031>
- Kayastha, R. B., Steiner, N., Kayastha, R., Mishra, S. K., & McDonald, K. (2020). Comparative Study of Hydrology and Icemelt in Three Nepal River Basins Using the Glacio-Hydrological Degree-Day Model (GDM) and Observations From the Advanced Scatterometer (ASCAT). *Frontiers in Earth Science*, 7, 354. <https://doi.org/10.3389/feart.2019.00354>
- Luis, A. J., Alam, M., & Jawak, S. D. (2022). Spatiotemporal change analysis for snowmelt over the Antarctic ice shelves using scatterometers. *Frontiers in Remote Sensing*, 3, 953733. <https://doi.org/10.3389/frsen.2022.953733>
- Nagler, T., & Rott, H. (2000). Retrieval of wet snow by means of multitemporal SAR data. *Geoscience and Remote Sensing, IEEE Transactions On*, 38, 754–765. <https://doi.org/10.1109/36.842004>
- Oza, S. R., Bothale, R. V., Ram Rajak, D., Jayaprasad, P., Maity, S., Thakur, P. K., Tripathi, N., Chouksey, A., & Bahuguna, I. M. (2019). Assessment of Cryospheric Parameters Over the Himalaya and Antarctic Regions using SCATSAT-1 Enhanced Resolution Data. *Current Science*, 117(6), 1002. <https://doi.org/10.18520/cs/v117/i6/1002-1013>
- Oza, S. R., Singh, R. K. K., Vyas, N. K., & Sarkar, A. (2011). Study of inter-annual variations in surface melting over Amery Ice Shelf, East Antarctica, using space-borne scatterometer data. *Journal of Earth System Science*, 120(2), 329–336. <https://doi.org/10.1007/s12040-011-0055-8>
- Panday, P. K., Frey, K. E., & Ghimire, B. (2011). Detection of the timing and duration of snowmelt in the Hindu Kush-Himalaya using QuikSCAT, 2000–2008. *Environmental Research Letters*, 6(2), 024007. <https://doi.org/10.1088/1748-9326/6/2/024007>
- Rau, F., Braun, M., Friedrich, M., Weber, F., & Goßmann, H. (2000). RADAR GLACIER ZONES AND THEIR BOUNDARIES AS INDICATORS OF GLACIER MASS BALANCE AND CLIMATIC VARIABILITY. 1.

Rawlins, M. A., McDonald, K. C., Frolking, S., Lammers, R. B., Fahnestock, M., Kimball, J. S., & Vörösmarty, C. J. (2005). Remote sensing of snow thaw at the pan-Arctic scale using the SeaWinds scatterometer. *Journal of Hydrology*, 312(1–4), 294–311. <https://doi.org/10.1016/j.jhydrol.2004.12.018>

Romshoo, S. A. (2004). Geostatistical analysis of soil moisture measurements and remotely sensed data at different spatial scales. *Environmental Geology*, 45(3), 339–349.
<https://doi.org/10.1007/s00254-003-0891-1>

Small, D. (2011a). Flattening Gamma: Radiometric Terrain Correction for SAR Imagery. *IEEE Transactions on Geoscience and Remote Sensing*, 49(8), 3081–3093.
<https://doi.org/10.1109/TGRS.2011.2120616>

Small, D. (2011b). Flattening Gamma: Radiometric Terrain Correction for SAR Imagery. *IEEE Transactions on Geoscience and Remote Sensing*, 49(8), 3081–3093.
<https://doi.org/10.1109/TGRS.2011.2120616>

Small, D. (2012). SAR backscatter multitemporal compositing via local resolution weighting. 2012 IEEE International Geoscience and Remote Sensing Symposium, 4521–4524.
<https://doi.org/10.1109/IGARSS.2012.6350465>

Trusel, L. D., Frey, K. E., & Das, S. B. (2012). Antarctic surface melting dynamics: Enhanced perspectives from radar scatterometer data. *Journal of Geophysical Research: Earth Surface*, 117(F2).
<https://doi.org/10.1029/2011JF002126>

Wang, L., Derksen, C., & Brown, R. (2008). Detection of pan-Arctic terrestrial snowmelt from QuikSCAT, 2000–2005. *Remote Sensing of Environment*, 112(10), 3794–3805.
<https://doi.org/10.1016/j.rse.2008.05.017>

Wang, L., Sharp, M. J., Rivard, B., Marshall, S., & Burgess, D. (2005). Melt season duration on Canadian Arctic ice caps, 2000–2004. *Geophysical Research Letters*, 32(19), 2005GL023962.
<https://doi.org/10.1029/2005GL023962>

Figures

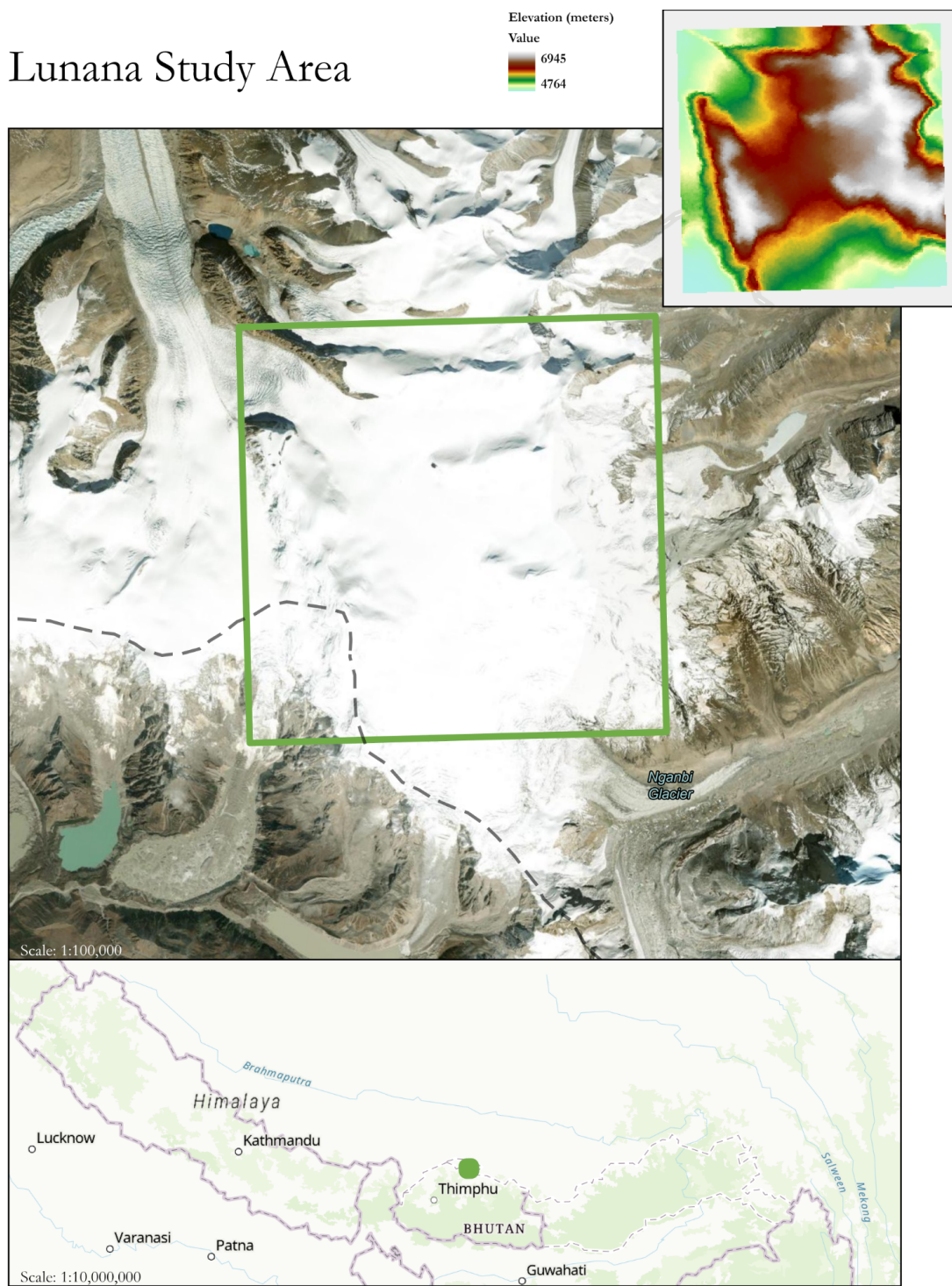


Figure 1: Lunana Study Area

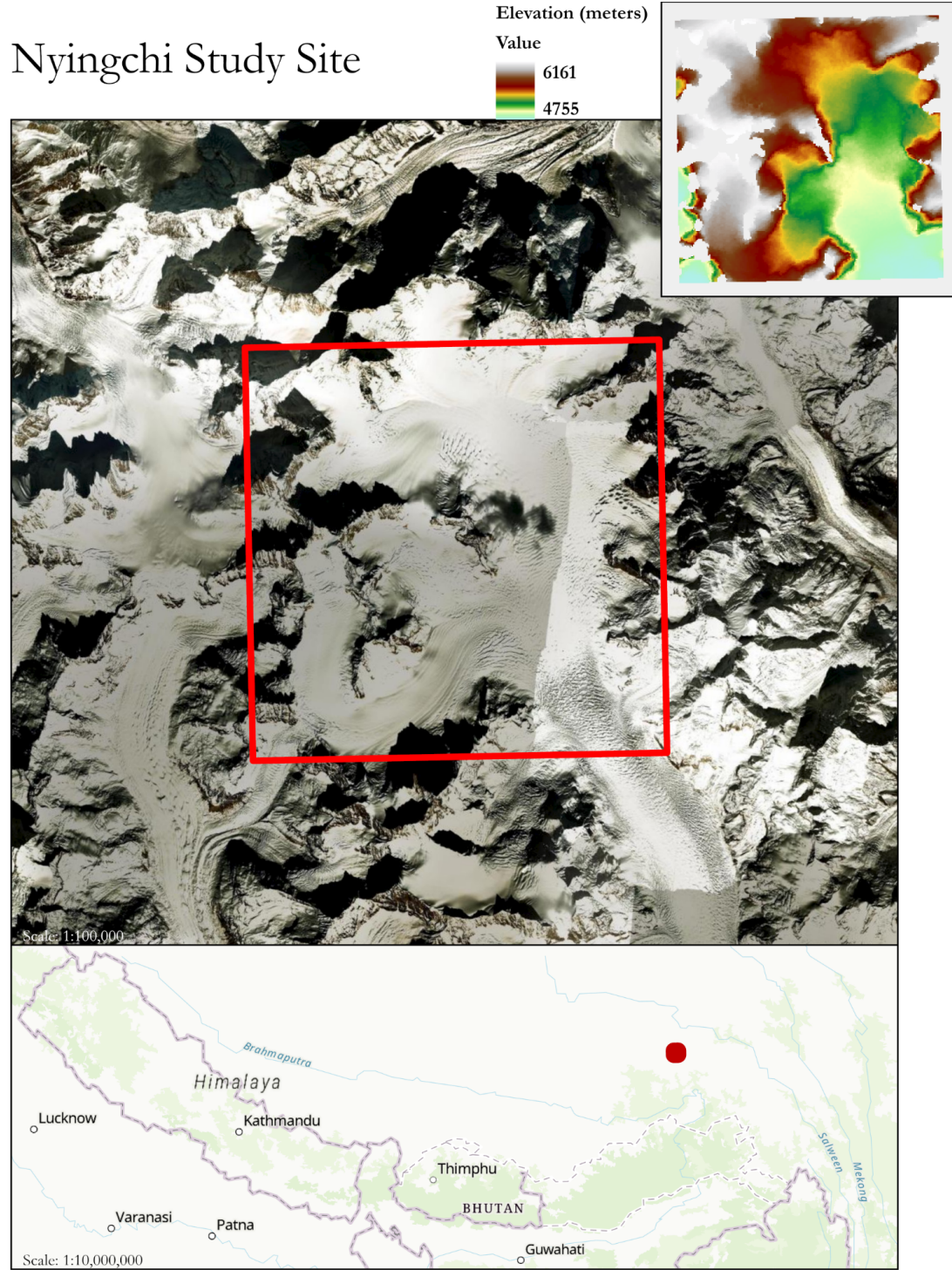


Figure 2: Nyingchi Study Site

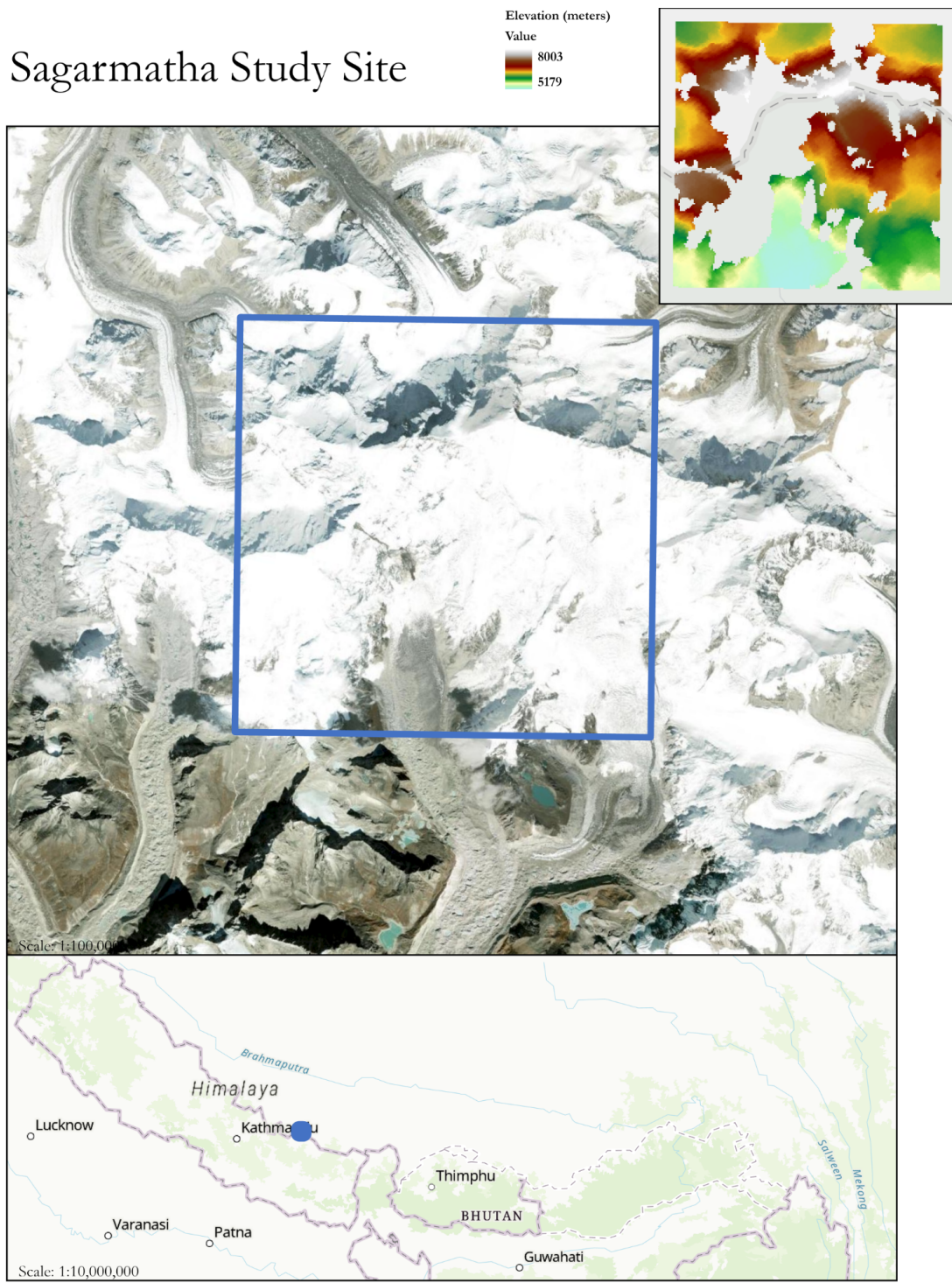


Figure 3: Sagarmatha Study Site

Site	AVG	16 Year	16 Year	Mean Max	Mean Min
	Elevation	Backscatter	Backscatter	Backscatter	Backscatter
	(meters)	Mean	Standard Deviation		
Lunana	6369	-2.6334	1.2838	-5.5718	-1.2768
Nyingchi	5287	-4.5267	1.2678	-6.4988	-2.6568
Sagarmatha	6273	-2.5781	0.7912	-4.1046	-1.4362

Figure 4: Study Site Summary Table

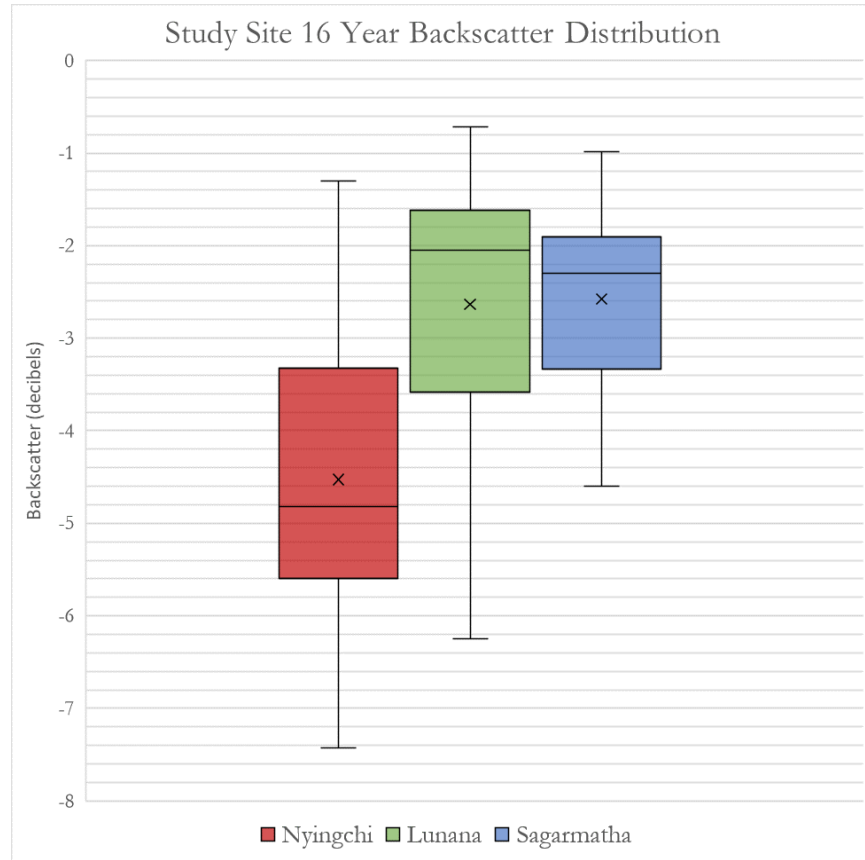


Figure 5: Study Site Variance Visualization

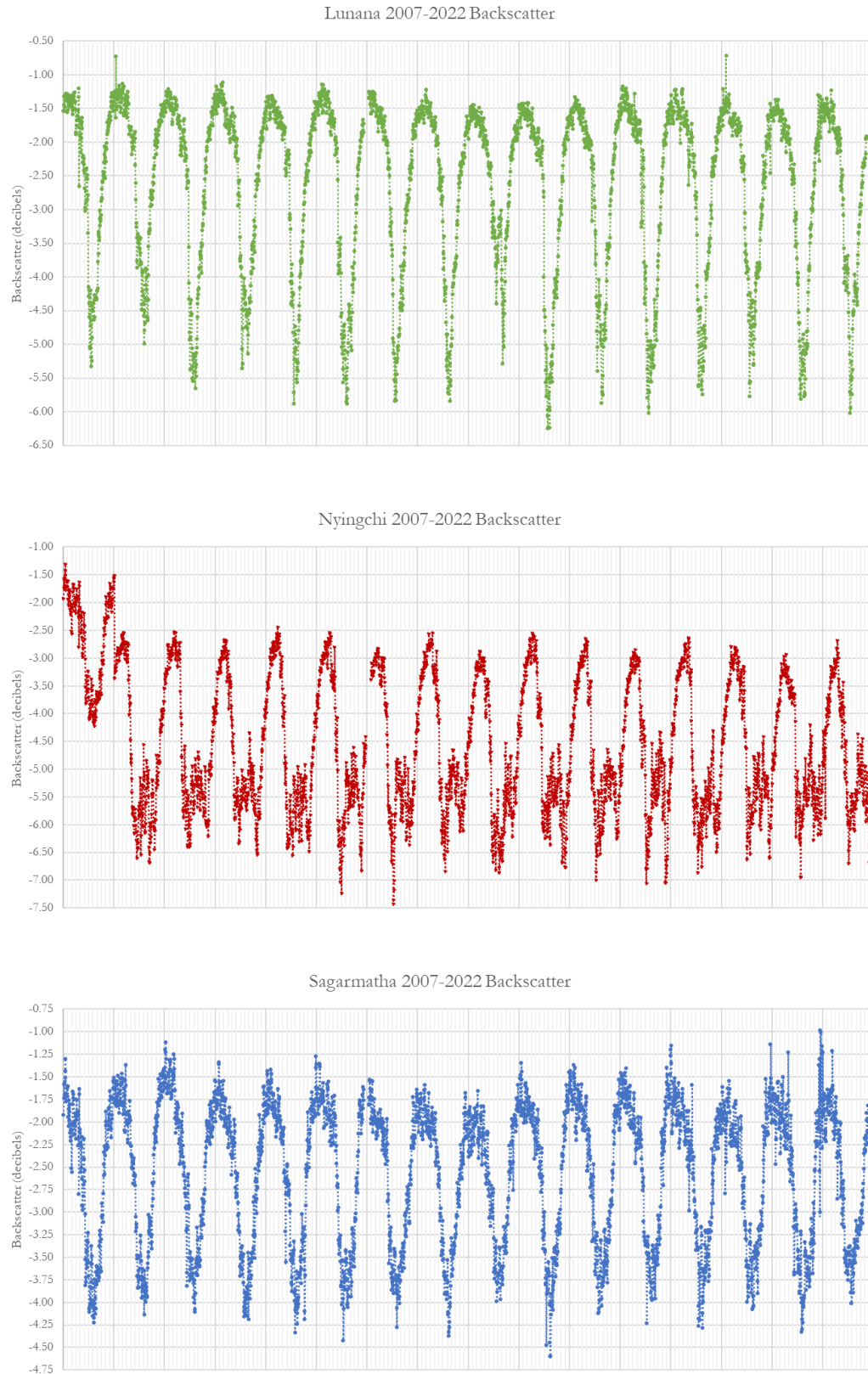


Figure 6: 16 Year Backscatter Plot

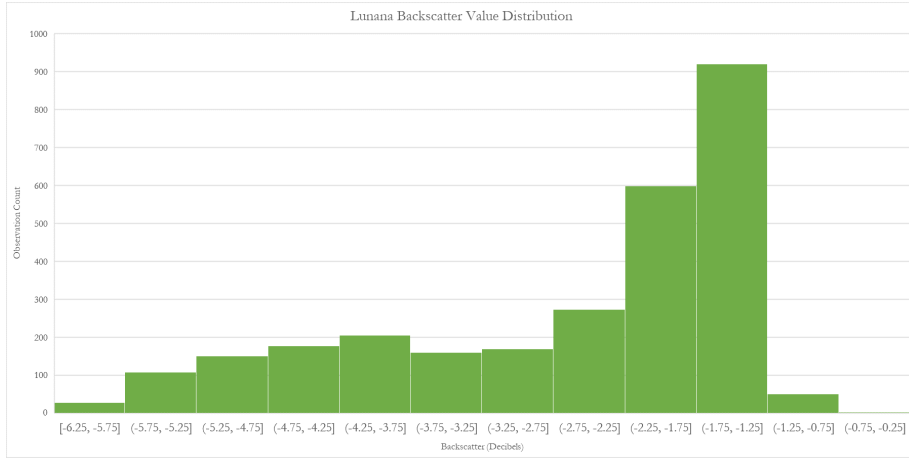


Figure 7: Lunana Backscatter Value Distribution

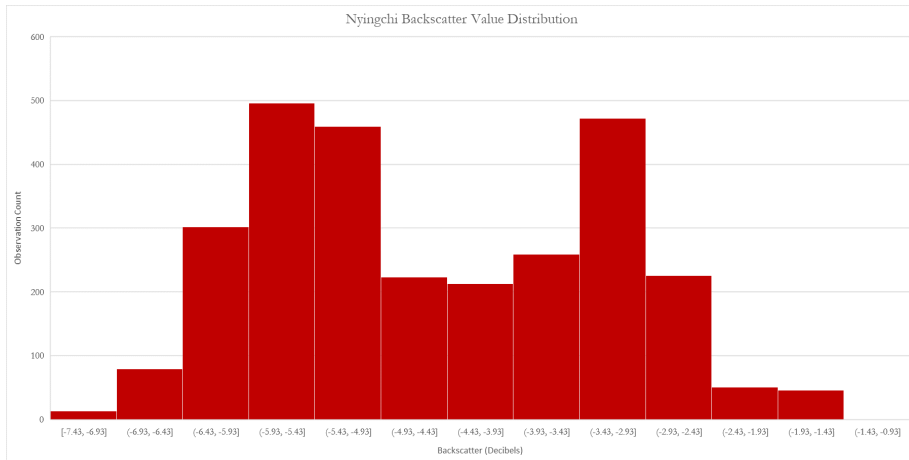


Figure 8: Nyingchi Backscatter Value Distribution

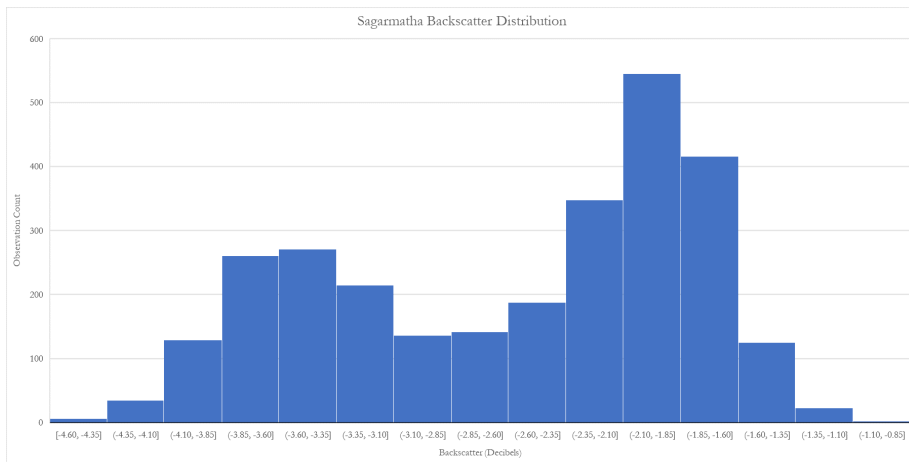


Figure 9: Sagarmatha Backscatter Value Distribution

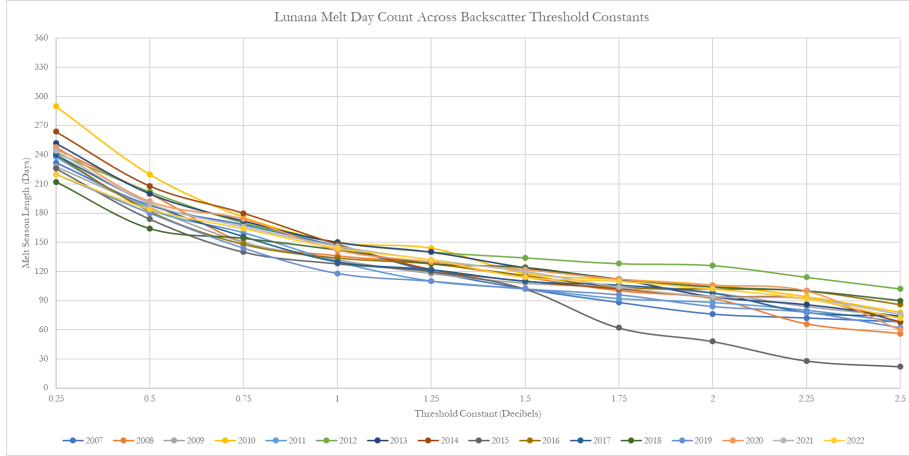


Figure 10: Lunana Melt Season Lengths Across Backscatter Threshold Constants

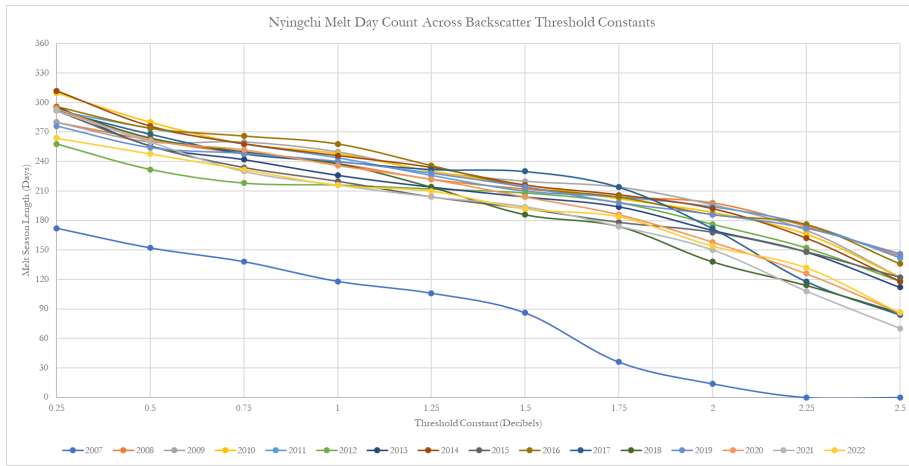


Figure 11: Nyingchi Melt Season Lengths Across Backscatter Threshold Constants

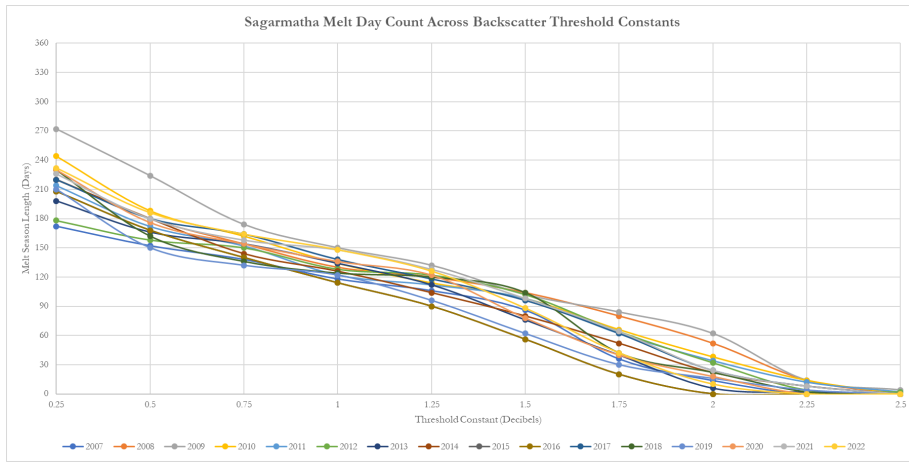


Figure 12: Sagarmatha Melt Season Lengths Across Backscatter Threshold Constants

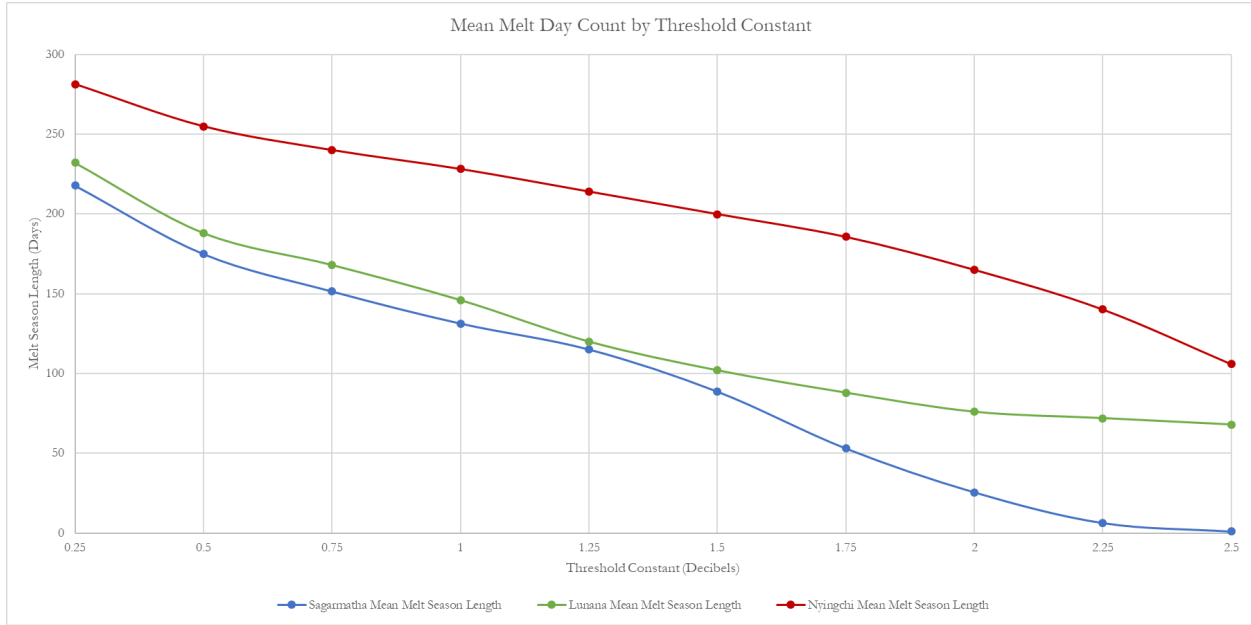


Figure 13: Mean Melt Season Length by Threshold Constant Across Sites



Figure 14: Melt Season Length Across Sites

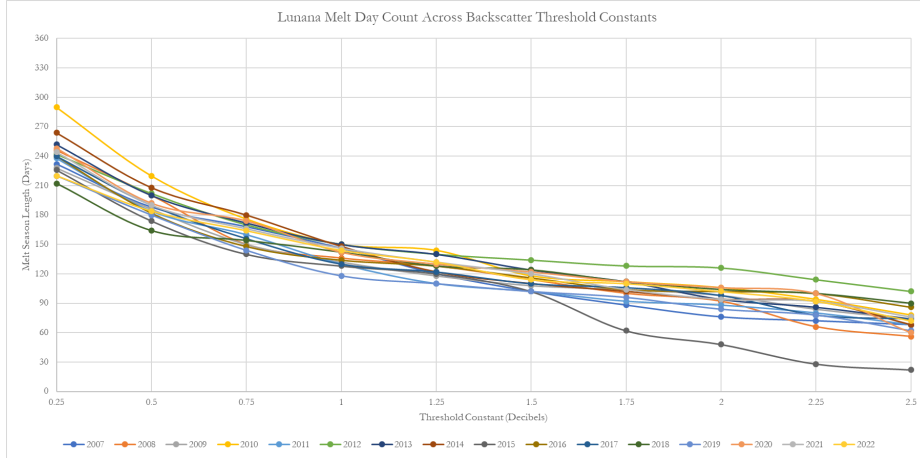


Figure 15: Lunana Melt Season Series

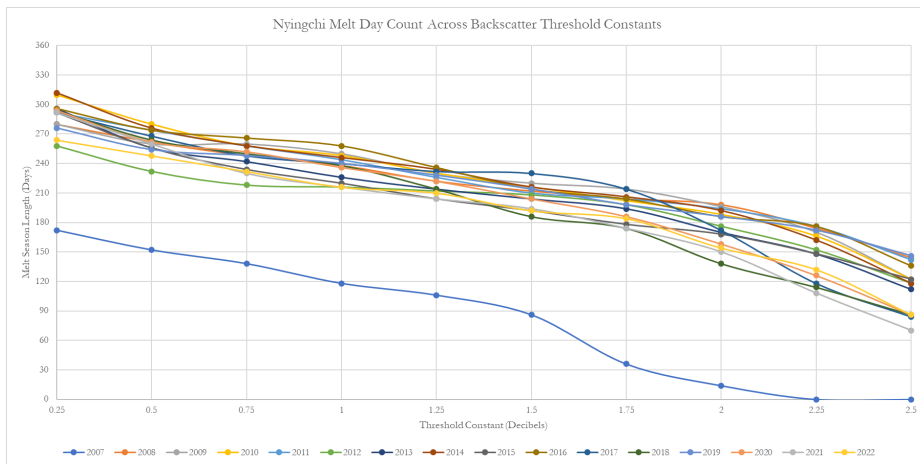


Figure 16: Nyingchi Melt Season Series

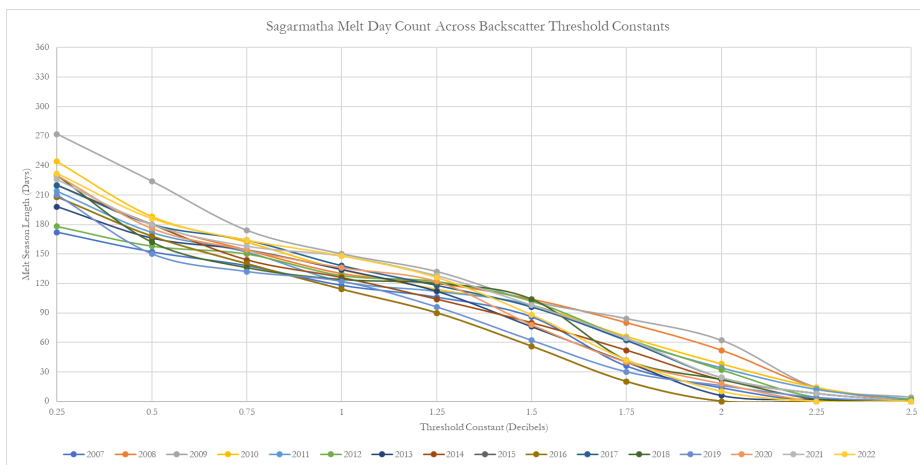


Figure 17: Sagarmatha Melt Season Series

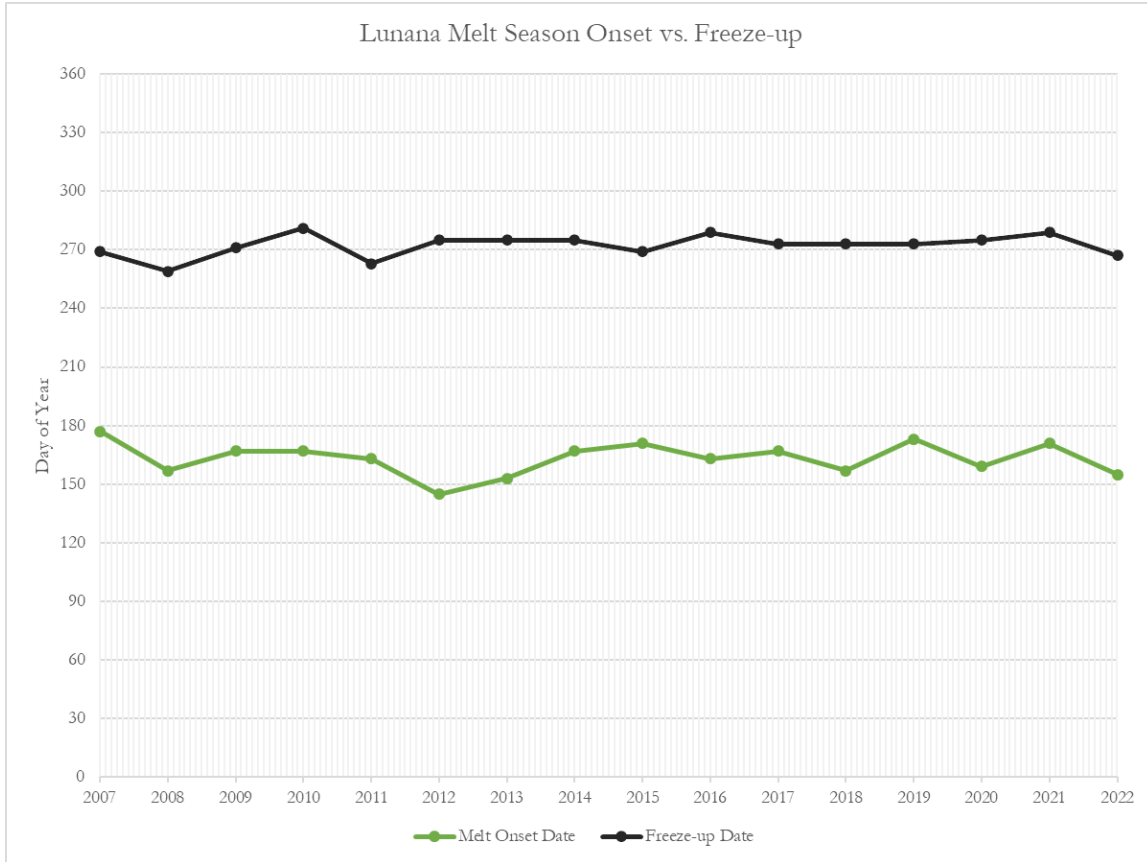


Figure 18: Lunana Melt Onset vs. Freeze Up Date

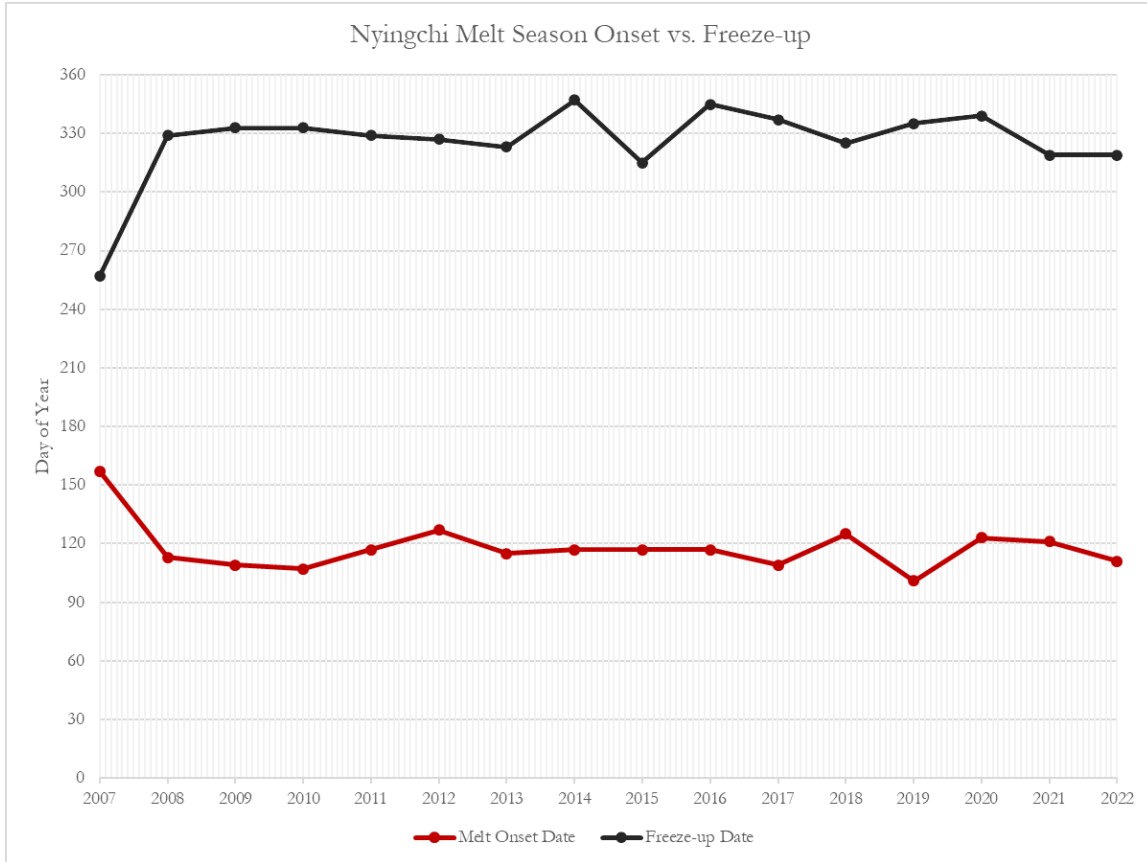


Figure 19: Nyingchi Melt Onset vs. Freeze-up Date

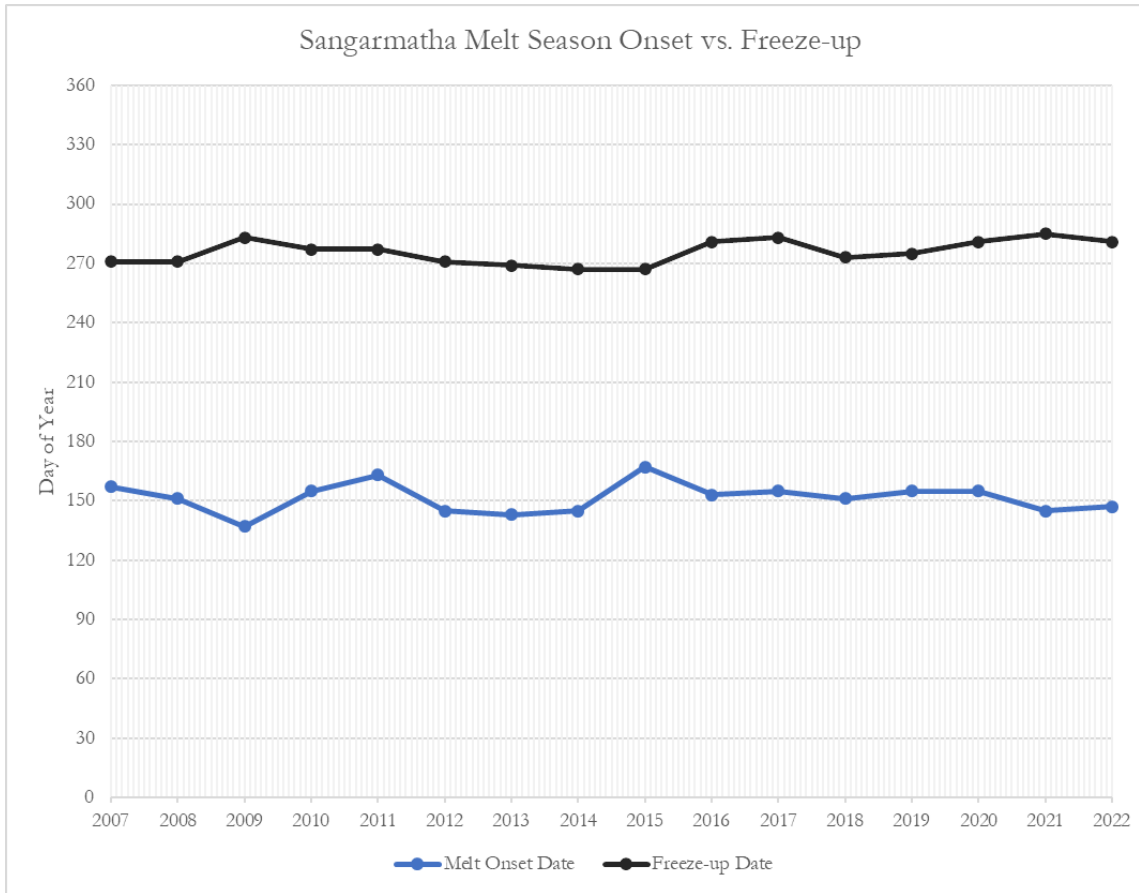


Figure 20: Sagarmatha Melt Onset vs. Freeze-up Date

Site	Melt Onset	Freeze-up	Mean Melt	Melt Onset	Freeze-up
	Day of Year	Day of Year	Season	Day of Year	Day of Year
	Mean	Mean	Length	Standard	Standard
Lunana	163	272	109	8.2	5.7
Nyingchi	118	326	208	12.1	19.8
Sagarmatha	152	276	124	7.4	5.9

Figure 21: Melt Onset and Freeze-up Day of Year Summary Statistics

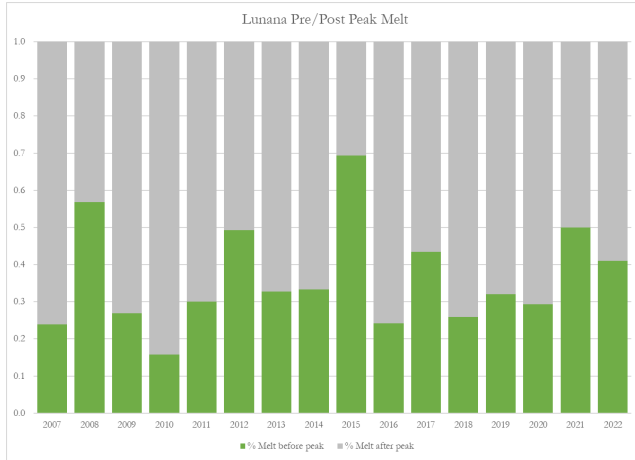


Figure 22: Lunana Percent of Melt Season Before and After Peak

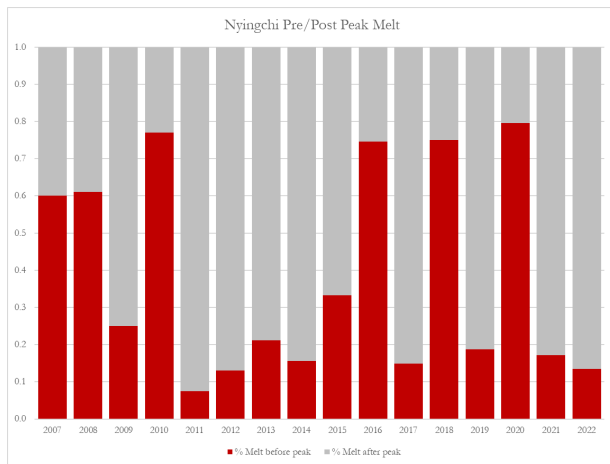


Figure 23: Nyingchi Percent of Melt Season Before and After Peak

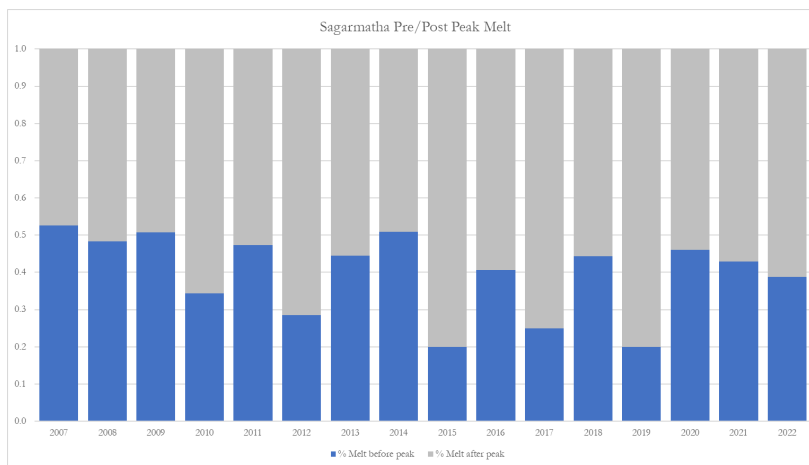


Figure 24: Sagarmatha Percent of Melt Season Before and After Peak

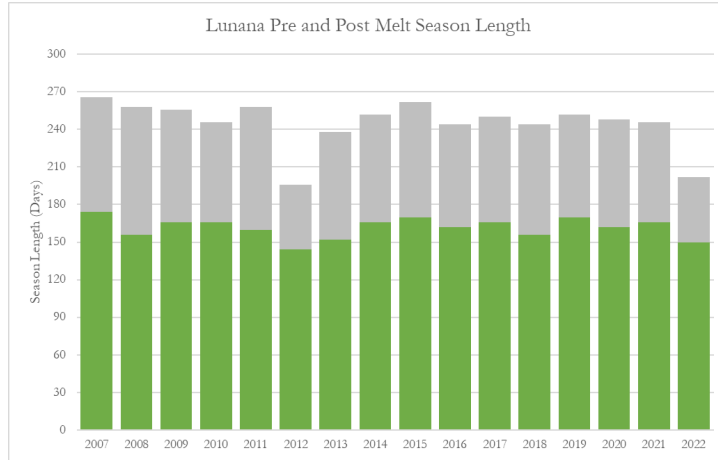


Figure 25: Lunana Pre and Post Melt Season Length

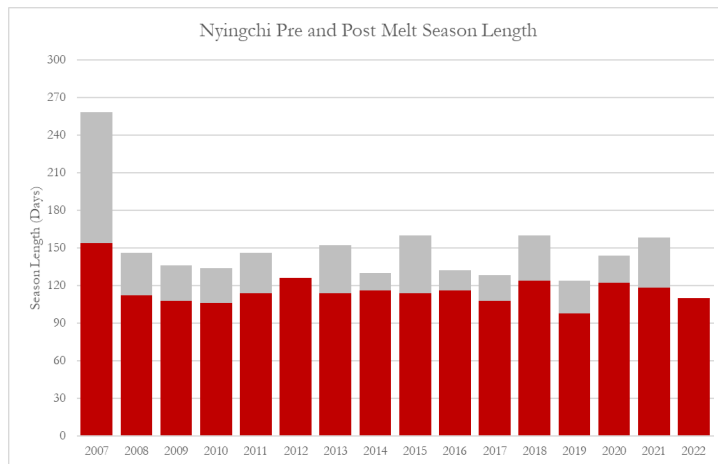


Figure 26: Nyingchi Pre and Post Melt Season Length

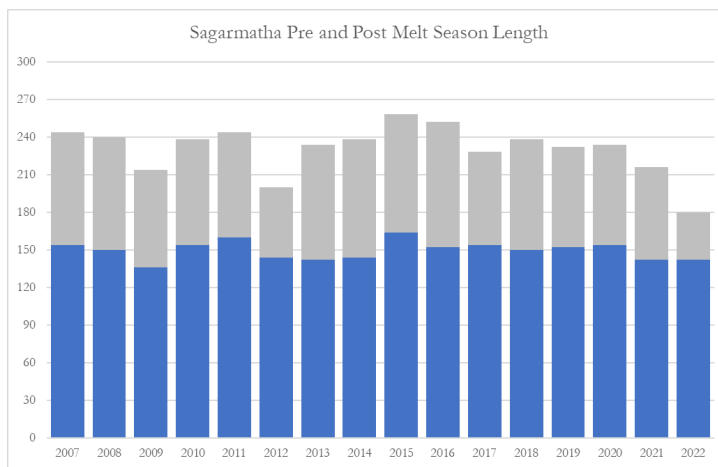


Figure 27: Sagarmatha Pre and Post Melt Season Length

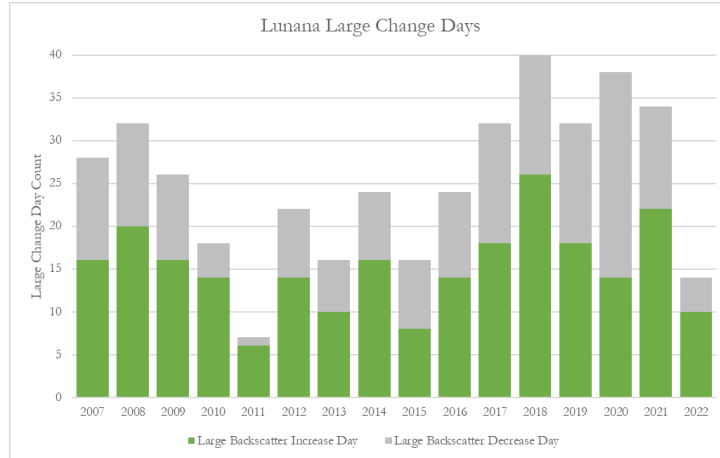


Figure 28: Lunana Days of Large Change

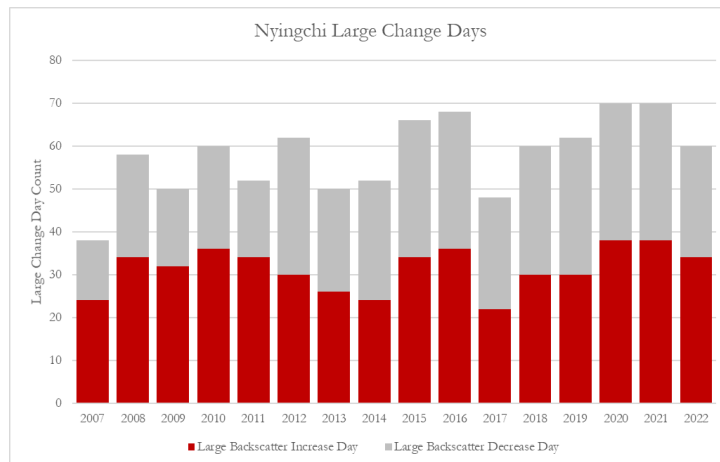


Figure 29: Nyingchi Days of Large Change

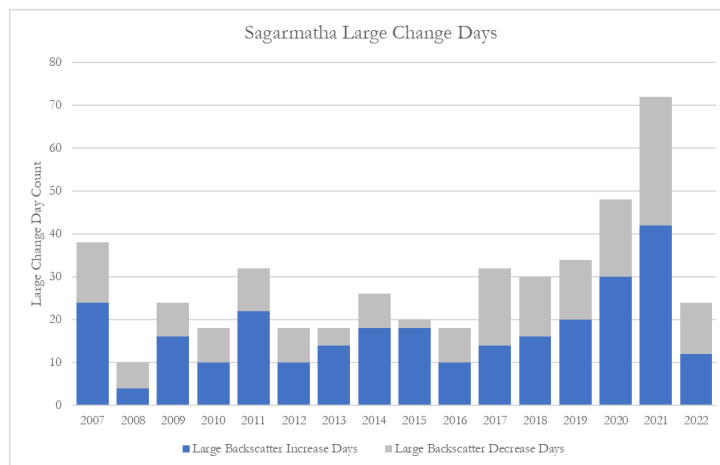


Figure 30: Sagarmatha Days of Large Change

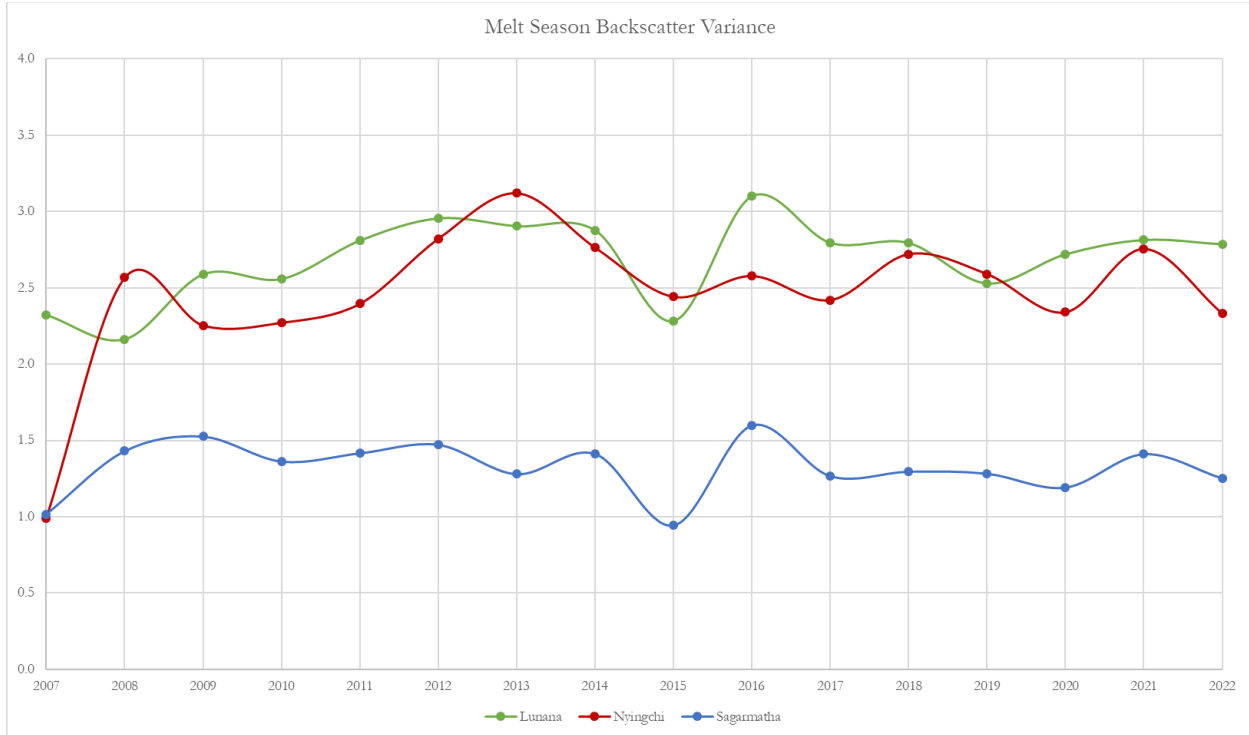


Figure 31: Melt Season Backscatter Variance Across Sites